

In Situ Atomic Force Microscopy Visualization of the Degradation of Melt-Crystallized Poly(sebacic anhydride)

K. M. Shakesheff, M. C. Davies,* A. Domb,[†] D. E. Jackson, C. J. Roberts,* S. J. B. Tendler,* and P. M. Williams

Laboratory of Biophysics and Surface Analysis, Department of Pharmaceutical Sciences, The University of Nottingham, University Park, Nottingham, NG7 2RD, U.K., and The Hebrew University of Jerusalem, School of Pharmacy, Jerusalem, 91120 Israel

Received July 18, 1994; Revised Manuscript Received October 13, 1994[®]

ABSTRACT: The surface degradation of melt-crystallized poly(sebacic anhydride) (PSA) has been visualized *in situ* in an aqueous environment using atomic force microscopy. The morphological changes accompanying degradation may be interpreted in terms of the preferential erosion of amorphous material revealing spherulitic crystalline features. The kinetics of polymer degradation were found to be pH dependent as anticipated and also dependent on the method of sample preparation, which influenced surface crystallinity. The future exploitation of *in situ* atomic force microscopy for the study of polymer degradation promises to provide a unique insight into the erosion process and enhance the current understanding of the relationship between polymer microstructure and erosion kinetics.

Introduction

The controlled release of drug molecules from biodegradable polymer matrices is an area of active research which promises many clinical and economic opportunities.^{1,2} Drug molecules within polymeric matrices are released from these devices as a consequence of the hydrolysis of labile chemical bonds in the polymer backbone. This results in the conversion of water-insoluble high molecular weight polymer chains into water-soluble low molecular weight products. Examples of polymers used in such devices include polyesters,³⁻⁵ polyamides,⁶ poly(ortho esters),⁷ and polyanhydrides.⁸

The polyanhydrides are a class of biodegradable polymers designed specifically for biomedical applications which are receiving considerable attention due to their predictable erosion.⁹⁻¹⁵ The general structure of a polyanhydride is shown in Figure 1 along with the mode of hydrolysis. The hydrolytic reactivity of an anhydride linkage is high, allowing biodegradation to be achieved with a wide variety of backbone structures. Surface erosion occurs due to the hydrophobicity of the polyanhydride backbone, which results in water penetration into the bulk being rate-limiting. The factors affecting polyanhydride hydrolysis have been discussed in the literature.^{16,17}

The success of backbone chemical modifications has yielded polymeric devices which release drug molecules *in vivo* over periods ranging from days to months. However, recently there has been an increased awareness that in designing novel biodegradable systems it is important to understand not only the effect of chemical composition on degradation kinetics but also the morphology and molecular organization of the polymeric material.^{18,19}

The influence of polymer morphology and molecular organization on the biodegradation of polyanhydride devices has been studied by a number of techniques including X-ray powder diffraction,¹⁸ differential scanning calorimetry (DSC),¹⁸ scanning electron microscopy (SEM), and optical microscopy.^{18,19} For poly(sebacic

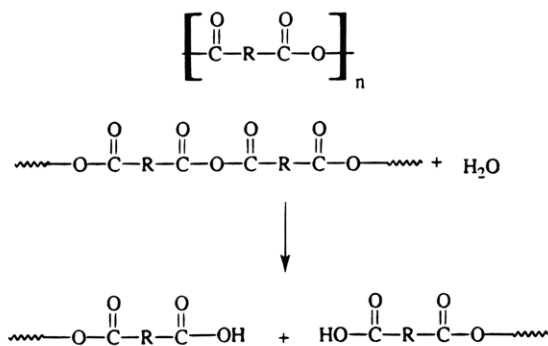


Figure 1. General structure of a polyanhydride and the mode of hydrolysis.

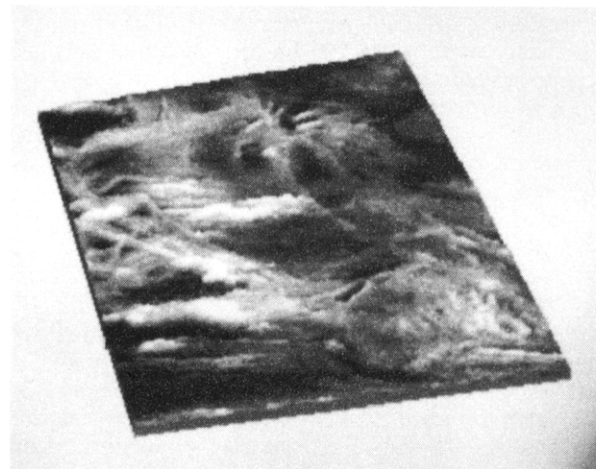


Figure 2. 13.2 μm × 13.2 μm AFM image displaying the presence of fibrous and smooth regions on the surface of melt-crystallized PSA samples. Gray scale image with height difference of 880 nm.

anhydride) (PSA) devices, these studies have revealed the semicrystalline nature of the material. X-ray powder diffraction has recorded the crystallite dimensions and DSC has provided quantitative data on the proportions of crystalline and amorphous regions within semicrystalline morphologies produced by both solvent and melt casting methods.

SEM and optical microscopy have provided visual data on the semicrystalline morphologies of PSA.¹⁹ With cross-polarized light microscopy the presence of

* To whom correspondence should be addressed at The University of Nottingham.

[†] The Hebrew University of Jerusalem.

[®] Abstract published in *Advance ACS Abstracts*, January 1, 1995.

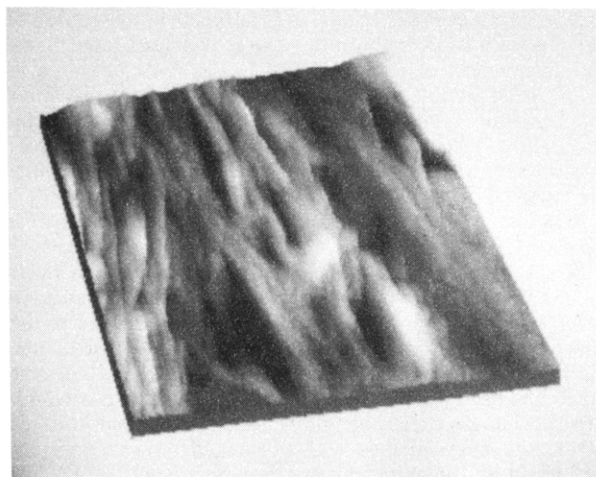


Figure 3. $3.3\ \mu\text{m} \times 3.3\ \mu\text{m}$ AFM image of a bundle of PSA fibers. Gray scale image with height difference of 326 nm.

Maltese cross patterns in thin films of PSA confirms the presence of spherulites, and the radiating fibrous structure of these spherulites has been observed using SEM. Upon degradation of these devices there is a loss of amorphous material between the fibers of the spherulites which is manifested in the electron micrographs by the observation of the dendritic skeleton. The preferential loss of amorphous material in the initial stages of PSA hydrolysis is attributed to the higher permeability of amorphous material over crystalline.

While SEM has provided valuable data on polyanhydride morphological changes, a major limitation is imposed by the need to coat the insulating PSA surfaces with a metallic film to enable the dissipation of electrons during imaging. Therefore, each polymer surface can only be analyzed by SEM at one time point in the degradation process and the effect of degradation on morphology has to be performed as a comparison of different samples. With the aim of overcoming some of the limitations of the SEM, we have utilized atomic force microscopy in the present study.

Atomic force microscopy is an attractive tool for studying polymer surface degradation and changes at the polymer/biological system interface. The technique can generate high-resolution three-dimensional topographies of naked (i.e., not coated), untreated, surfaces and may be employed in a variety of imaging environments.²⁰ Atomic force microscopy has previously been used to image the molecular organization of polymeric surfaces, as demonstrated, for example, in the differentiation of α - and γ -contact faces of isotactic polypropylene²¹ and the imaging of polyethylene molecules in extended chain crystals.²²

The ability of the AFM to image naked materials in a range of imaging environments has allowed the technique to be utilized in the study of interactions at interfaces. Examples of such studies include the adsorption of molecules to a zeolite surface,²³ the real-time imaging of the clotting of human blood protein fibrinogen,²⁰ the adsorption of IgG and glucose oxidase to

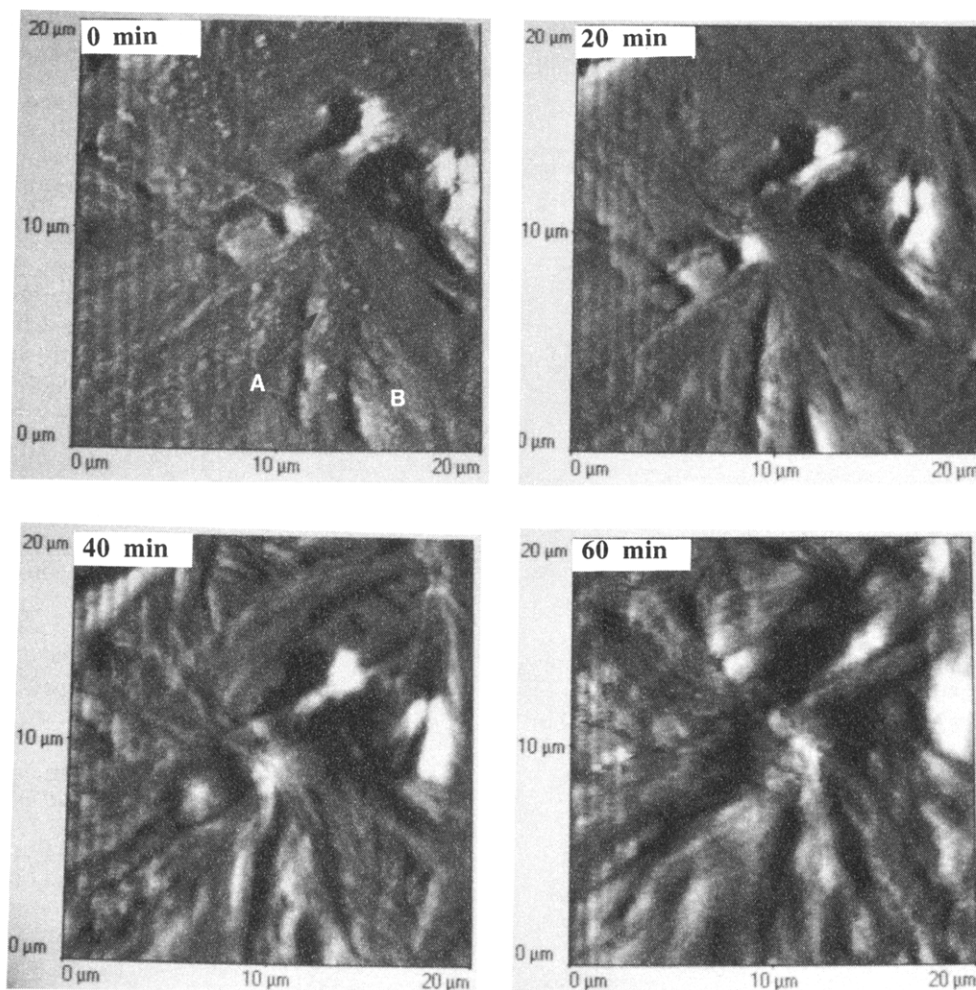


Figure 4. *In situ* AFM images ($20\ \mu\text{m} \times 20\ \mu\text{m}$) of the degradation of melt-crystallized PSA in a pH 12.5 NaOH aqueous solution.

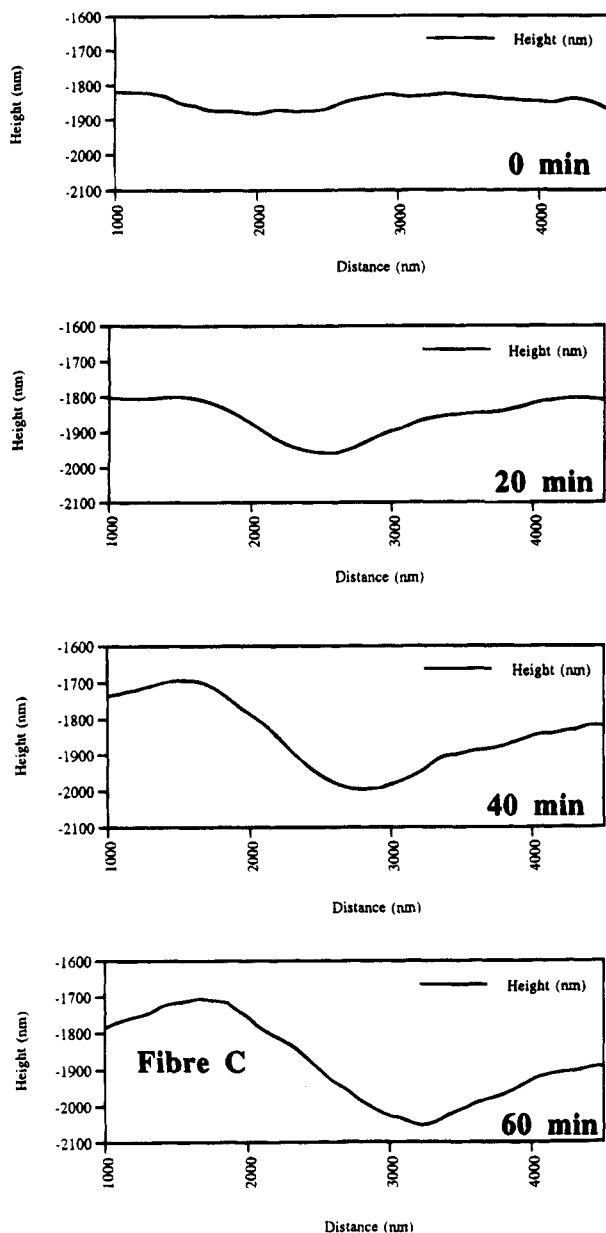


Figure 5. Cross-sectional height detail for line A–B in Figure 4 displaying the exposure of the fiber C with time.

mica,²⁴ and the budding of a virus from an infected cell.²⁵

In this paper, we describe a new example of the atomic force microscopy of interface interactions. We have utilized *in situ* atomic force microscopy in the study of polyanhydride surface erosion. The devices analyzed consist of melt-crystallized PSA, a system which has been well characterized by SEM^{18,19} and other techniques. First, we have characterized the surface morphology of the samples; then morphological changes occurring during degradation have been recorded within an aqueous environment on untreated PSA surfaces. It has also been possible to demonstrate the effect of the pH of the environment on the degradation kinetics.

Experimental Section

PSA, $M_w = 25\,000$, was synthesized by polycondensation as described previously.²⁶ Samples for AFM analysis were prepared by melting the polymer at 86 °C and then cooling slowly over a predetermined time period.

Surface morphology characterization was performed using a Polaron SP300 AFM (VG Microtech, Uckfield, U.K.) in air

with a 30 μm scanner head. Si_3N_4 probes on triangular cantilevers were used to obtain images in constant-force mode at scan frequencies of between 5 and 10 Hz. Data obtained with the Polaron SP300 is presented as gray scale topographs in which height information is represented by the pixel shade. The height difference quoted with each image refers to the vertical separation between the lowest and highest point on the topograph.

In situ atomic force microscopy and degradation experiments were performed with a Topometrix TMX 2000 Explorer AFM (J.K. Instruments LTD., Saffron Walden, Essex, U.K.) with a 150 μm scanner head employing the same imaging parameters as for the surface morphology characterization. When using this instrument, samples were initially analyzed in air to characterize the surface morphology. Then distilled water, which had been passed through a 0.2 μm filter, was introduced into the imaging chamber and after 1 h of exposure to the water, the PSA surface was re-imaged. Degradation was performed by replacing the water with a NaOH(aq) solution of known pH or a pH 7.4 phosphate buffer solution, all these solutions having been filtered prior to use. AFM images were then recorded at regular intervals. *In situ* images are presented in shaded view.

Results and Discussion

Surface characterization of the melt-crystallized PSA revealed a fibrous morphology typical of a semicrystalline polymer. The 13.2 $\mu\text{m} \times 13.2 \mu\text{m}$ AFM image in Figure 2 is an example of this morphology. Fibers with diameters in the range of 50–200 nm were present in bundles on some areas of the surface. One such area is imaged in the 3.3 $\mu\text{m} \times 3.3 \mu\text{m}$ AFM topograph in Figure 3, where an interwoven network of PSA fibers is evident. However, other areas of the surface had a smooth texture indicative of amorphous polymeric material. This type of surface morphology, consisting of crystalline fibrous and amorphous smooth regions, is consistent with morphologies observed by SEM^{18,19} and has been well documented in the literature.²⁷

An important sample preparation factor in determining the morphology was the cooling rate during solidification. If during the cooling of the PSA melt the oven temperature was held at 70 °C (10 °C above the glass transition temperature T_g) for 10 min, the proportion of fibers at the surface increased and often spherulitic structures could be observed. From extensive transmission electron microscopy (TEM) studies performed mainly on polyethylene spherulites, it is known that spherulites are composed of chain fold lamellae which form crystallites which are then organized into fibers. Amorphous material which failed to crystallize during solidification is present between the fibers.²⁷ By increasing the rate of cooling during solidification it was possible to inhibit the formation of spherulites in the PSA samples. The surface morphology for these samples consisted of a granular texture.

Having characterized the surface morphology of the PSA prior to degradation, a study was then performed to ensure that the AFM imaging process did not induce morphological changes at the polymer surface. A 5 day experiment was performed in which a PSA surface was imaged in a pH 7 aqueous environment. During this period AFM images were recorded initially every 30 min and then at 6 hourly intervals. At pH 7, the degradation rate of these densely packed surfaces is negligible and therefore any morphological changes observed would have to be attributed to the action of the AFM probe. However, no perceivable changes in polymer surface structure were recorded over the 26 scans.

In situ degradation studies were then performed in a pH 12.5 aqueous environment in which the hydrolysis

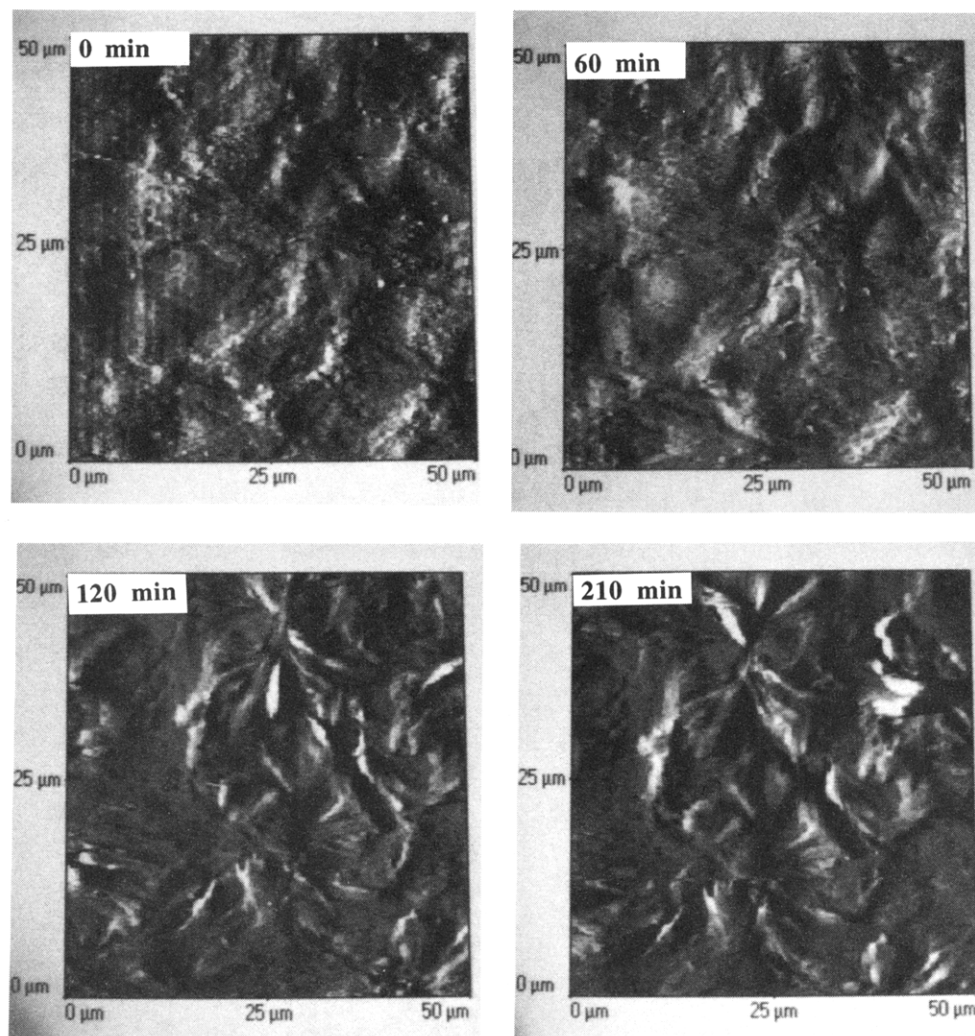


Figure 6. *In situ* AFM images ($50\ \mu\text{m} \times 50\ \mu\text{m}$) of degradation at pH 11.5.

of the anhydride linkage is enhanced. This enabled morphological changes to be recorded over short periods of time, allowing a large number of repeats to be performed and instrumental variables to be optimized.

Four $20\ \mu\text{m} \times 20\ \mu\text{m}$ AFM images are shown in Figure 4, which demonstrate the change in surface morphology occurring due to degradation following the exposure of a surface to the pH 12.5 NaOH solution. This sample was prepared with a 10 min delay period at $70\ ^\circ\text{C}$. The data clearly demonstrate an etching of the surface due to the preferential loss of the amorphous PSA material. This results in the exposure of fibrous, crystalline material. After 20 min of exposure to the alkaline solution a number of elongated indentations can be observed on the surface due to the loss of amorphous material between fibers. These indentations widen and deepen as the exposure time increases. In Figure 5, four cross-sections are presented taken from the positions marked A to B on Figure 4. These cross-sections highlight the etching of the surface as demonstrated by the fiber for which there is a relative increase in exposure height from 70 nm at time 9 min, to 150 nm at 20 min, to 300 nm at 40 min, and then 350 nm at 60 min. There is a very slight drift in the z -height of the cross-sections; therefore relative heights have been measured as the difference between the maximum and minimum heights on the cross-section. The change in surface morphology follows the same pattern observed in SEM studies.^{18,19} However, using the AFM it has

been possible to follow the degradation in real time on one area of the sample and to obtain vertical height data.

The pH dependence of the hydrolysis of the polyanhydride has been demonstrated by other techniques and was an important goal in the analysis using *in situ* atomic force microscopy. The series of $50\ \mu\text{m} \times 50\ \mu\text{m}$ AFM images shown in Figure 6 were recorded during a degradation experiment performed in a pH 11.5 NaOH solution, using a sample prepared in a similar manner to that imaged in Figure 4. A similar pattern of degradation is observed in this data as seen at pH 12.5. However, the kinetics of the degradation are, as expected, considerably slowed. Hence, the clear appearance of fibrous material at the surface due to preferential loss of amorphous PSA is noticeable over a period of 2–3.5 h at the lower pH. Degradation experiments have also been performed at lower pH values with corresponding lower degradation kinetics. At pH 7.4, the initial loss of amorphous material is initially observed after approximately 24 h.

Our experiments have also shown that sample preparation and its influence on surface crystallinity have an effect on surface degradation. The AFM images in Figure 7 show a degradation experiment performed at pH 12.5 on a sample cooled rapidly during solidification. The surface displays no spherulitic or fibrous morphology. However, the AFM images recorded after 20 and 90 min contact with the alkaline solution demonstrate

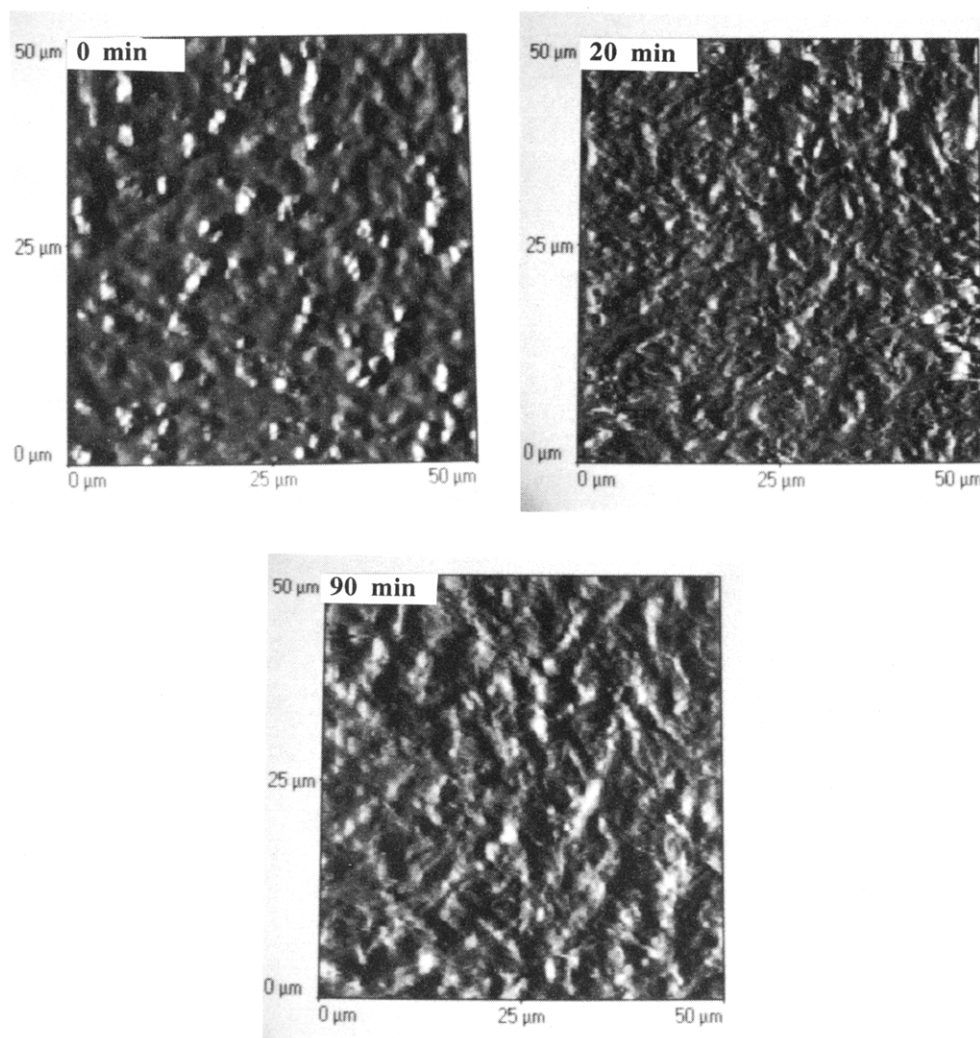


Figure 7. *In situ* AFM images ($20\ \mu\text{m} \times 20\ \mu\text{m}$) of the degradation of a rapidly cooled melt-crystallized PSA sample in a pH 12.5 NaOH aqueous solution.

the exposure of subsurface crystalline material. It appears, therefore, that these PSA melt-crystallized samples possess more amorphous material at the surface. The rapid solidification of the sample has prevented the formation of spherulites at the surface.

In the development of new applications of scanning probe microscopes, data validation is essential due to the close relationship between the sample surface and the scanning probe when the instrument is operated in contact mode. A number of groups have recorded morphological changes as a result of the action of an AFM probe on polymer surfaces.^{28,29} In the studies we perform on polymer surface degradation, in which we are observing morphological changes due to hydrolysis, it is important that we eliminate the possibility of the erroneous results due to tip-surface interactions. As stated above, prior to performing degradation we ensured the imaging process did not disrupt the PSA surface by imaging for 5 days in a pH 7 environment. However, during the accelerated degradation experiments, the hydrolytic process could change the mechanical properties of the PSA surface and, therefore, it was necessary to develop a method a self-validation which could be performed during the experiment. For this purpose, during all degradation experiments a protocol was adopted by which following the acquisition of a $20\ \mu\text{m} \times 20\ \mu\text{m}$ AFM image, a $50\ \mu\text{m} \times 50\ \mu\text{m}$ AFM image

was recorded. This large scan contained the smaller scan area. Now, if the action of the probe scanning the sample surface accelerated the degradation process, the central $20\ \mu\text{m} \times 20\ \mu\text{m}$ area of the $50\ \mu\text{m} \times 50\ \mu\text{m}$ image would display a larger morphological change than the surrounding area, due to the larger extent of interaction with the AFM probe during previous scans. Similarly, if the probe inhibits degradation, the central region would display less morphological change. The series of $50\ \mu\text{m} \times 50\ \mu\text{m}$ AFM images in Figure 8 were taken after the data shown in Figure 4 during a degradation at pH 12.5. From this data it can be observed that the central $20\ \mu\text{m} \times 20\ \mu\text{m}$ area of these images has undergone similar degrees of morphological changes. Therefore, we conclude that over the time scale of these experiments the AFM probe did not influence the surface morphology at the micron-scale level.

As a final step in our analysis, we have performed preliminary studies in which the three-dimensional data from the AFM is used to calculate volume changes occurring to the polymer film as a result of surface erosion. The calculations have been performed on the Genesis II molecular graphics system.³⁰ One problem which must be overcome in these calculations is the instrumental drift in the recorded height of the AFM data. The approach we have chosen to eliminate the problems of drift involves identifying a fiber on the scan area which is present in all the images taken through-

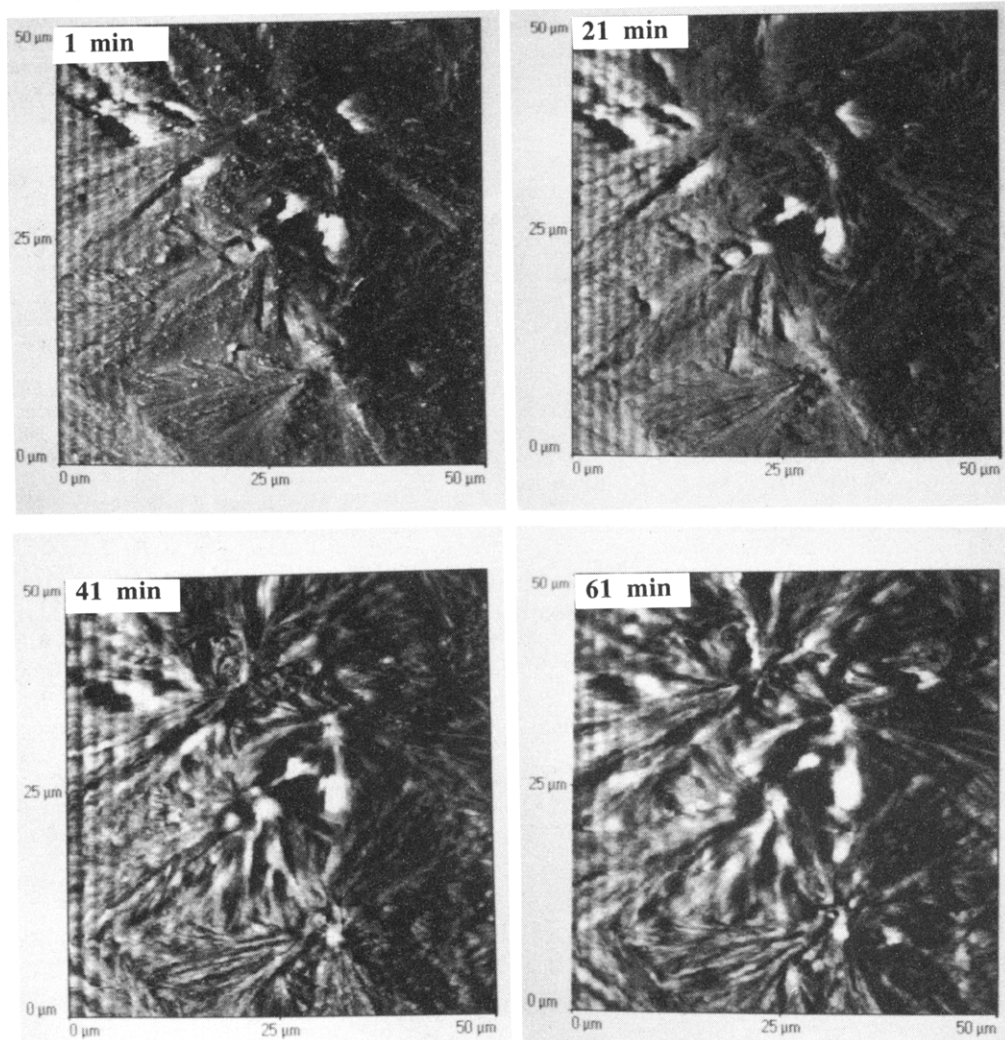


Figure 8. 50 μm \times 50 μm validation AFM images taken from areas shown in Figure 4.

out the degradation experiment. It is then assumed that the real maximum height of this fiber is unchanged through the course of the experiment. This assumption is reasonable while the rate of degradation of amorphous material greatly exceeds the rate of degradation of the crystalline fibers. The maximum recorded height of the fiber can then be used as a reference point to which the calculated volumes of the AFM images can be adjusted; hence instrumental drift is removed from the height data. Using the adjusted volumes, it is then possible to calculate the relative volume changes as the erosion occurs.

For the AFM data displayed in Figure 8, we have calculated the total change in the volume of the polymer matrix as a result of the erosion. The volumes were calculated from the central 30 μm \times 30 μm area of the scans. The volume difference between the images at 1 and 61 min of exposure to the pH 12.5 solution was found to be 333 μm^3 . The same calculation was then performed on the data in Figure 6 which had been recorded at pH 11.5. For this data, the total volume change over the 210 min degradation time was 144 μm^3 , demonstrating the slower rate of hydrolysis in the lower pH aqueous solution.

The volume analysis results presented are at a preliminary stage and have been included to demonstrate the potential of the AFM in the measurement of volume changes. They indicate that the kinetics of polymer loss during erosion may be quantified using the

AFM. Current studies are employing computational and instrumental methods to validate this method of volume analysis for biodegradable polymer systems.

Conclusions

In situ atomic force microscopy performed in aqueous conditions has enabled the visualization of the degradation of melt-crystallized PSA surfaces. This has facilitated the observation of a surface etching effect in which amorphous material is rapidly lost, resulting in an increased crystallinity of the exposed surface. Furthermore, by varying the pH of the imaging environment, we have demonstrated the pH dependence of the catalysis of hydrolysis.

The cooling rate employed during the solidification of the samples influences the microstructure. Rapid cooling prevents spherulite formation and results in a granular surface morphology. Upon degradation of the granular surface a fibrous morphology is revealed, suggesting a higher content of amorphous material at the surface.

We believe that these results provide further evidence of the developing role of *in situ* atomic force microscopy in the study of biomaterials. In the design of controlled drug delivery systems using surface-degrading polymers, *in situ* AFM can provide an explanation of the influence of polymer microstructure on the degradation process and hence the drug release kinetics.

Acknowledgment. The authors would like to acknowledge the BRITE EURAM program and the EPSRC/DTI Nanotechnology LINK Initiative with Kodak Limited, Oxford Molecular Group plc, and VG Microtech for funding these studies.

References and Notes

- (1) Leong, K. W.; Langer, R. *Adv. Drug Delivery Rev.* **1987**, *1*, 199.
- (2) Langer, R. *Science* **1990**, *249*, 1527.
- (3) Domb, A. J.; Amselem, S.; Maniar, M. In *Polymeric Biomaterials*; Dumitriu, S., Ed.; Marcel Dekker, Inc.: New York, 1994; Chapter 13.
- (4) Holland, S. J.; Tighe, B. J.; Gould, P. L. *J. Controlled Release* **1986**, *4*, 155.
- (5) Vert, M.; Li, S. M.; Garreau, H. *J. Controlled Release* **1991**, *16*, 15.
- (6) Heller, J. *J. Controlled Release* **1985**, *2*, 167.
- (7) Leong, K. W.; Kost, J.; Mathiowitz, E.; Langer, R. *Biomaterials* **1986**, *7*, 364.
- (8) Tamada, J.; Langer, R. *Macromolecules* **1992**, *3*, 315.
- (9) Mathiowitz, E.; Langer, R. *J. Controlled Release* **1987**, *5*, 13.
- (10) Mathiowitz, E.; Ron, E.; Mathiowitz, G.; Langer, R. *Macromolecules* **1993**, *26*, 6754.
- (11) Mathiowitz, E.; Amato, C.; Dor, Ph.; Langer, R. *Polymer* **1990**, *31*, 547.
- (12) Mathiowitz, E.; Saltzman, W. M.; Domb, A.; Dor, Ph.; Langer, R. *J. Appl. Polym. Sci.* **1988**, *35*, 755.
- (13) Grossman, S. A.; Reinhard, C.; Colvin, O. M.; Chasin, M.; Brundrett, R.; Tamargo, R. J.; Brem, H. *J. Neurosurg.* **1992**, *76*, 640.
- (14) Tabata, Y.; Gutta, S.; Langer, R. *Pharm. Res.* **1993**, *10*, 487.
- (15) Brem, H. *Biomaterials* **1990**, *11*, 699.
- (16) Domb, A. J.; Nudelman, R. *Biomaterials*, in press.
- (17) Domb, A. J.; Amselem, S.; Shah, J.; Maniar, M. In *Synthesis and Characterization in Advances in Polymer Science*; Langer, R., Pepass, N., Eds.; Springer-Verlag: Berlin, 1993; Vol. 107, pp 95-141.
- (18) Göpferich, A.; Langer, R. *J. Polym. Sci., Part A: Polym. Chem.* **1993**, *31*, 2445.
- (19) Mathiowitz, E.; Jacob, J.; Pekarek, K.; Chickering, D., III. *Macromolecules* **1993**, *26*, 6756.
- (20) Drake, B.; Prater, C. B.; Weisenhorn, A. L.; Gould, S. A. C.; Albrecht, T. R.; Quate, C. F.; Cannell, D. S.; Hansma, H. G.; Hansma, P. K. *Science* **1989**, *243*, 1586.
- (21) Stocker, W.; Magonov, S. N.; Cantow, H. J.; Wittman, J. C.; Lotz, B. *Macromolecules* **1993**, *26*, 5915.
- (22) Annis, B. K.; Reffner, J. R.; Wunderlich, B. *J. Polym. Sci., Part B* **1993**, *31*, 93.
- (23) Weisenhorn, A. L.; MacDougall, J. E.; Gould, S. A. C.; Cox, S. D.; Wise, W. S.; Massie, J.; Maivald, P.; Elings, V. B.; Stucky, G. D.; Hansma, P. K. *Science* **1990**, *247*, 1330.
- (24) Cullen, D. C.; McKerr, G.; Hughes, E. M. *Microsc. Anal.* **1993**, *37*, 31.
- (25) Häberle, W.; Hörber, F.; Ohnesorge, F.; Smith, D. P. E.; Binnig, G. *Ultramicroscopy* **1992**, *42-44*, 1161.
- (26) Domb, A. J.; Langer, R. *J. Polym. Sci., Part A: Chem. Ed.* **1991**, *42*, 1597.
- (27) Bassett, D. C. *CRC Crit. Rev. Solid State Mater. Sci.* **1984**, *12*, 97.
- (28) Meyers, G. F.; DeKoven, B. M.; Seitz, J. T. *Langmuir* **1992**, *8*, 2330.
- (29) Jin, X.; Unerti, W. N. *Appl. Phys. Lett.* **1992**, *61*, 657.
- (30) Williams, P. M.; Davies, M. C.; Jackson, D. E.; Roberts, C. J.; Tendler, S. J. B.; Wilkins, M. J. *Nanotechnology* **1991**, *2*, 998.

MA941115O